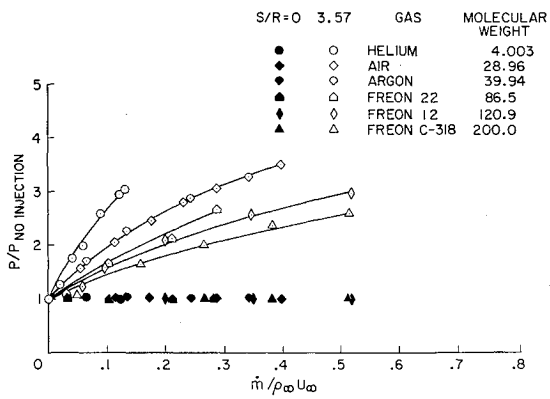

Fig. 6 Effect of injection gas on pressure distribution.

consider the effects of freestream density and nose radius in its formulation; therefore, the low-density flow of the present tests can be adequately represented by the theory.

The relative reduction in heat transfer measured on the afterbody due to injection of the various gases is similar to that in Fig. 5. The freon gases show the same heat reduction effectiveness.

The effect of the molecular weight of the injected gas on the surface pressure at the stagnation point and a representative point on the afterbody is shown in Fig. 6. At the stagnation point, molecular weight and rate of mass addition have no effect on the surface pressure. On the afterbody, molecular weight and injection rate have a very strong effect on surface pressure. Note that the freon gases have the expected individual effect of molecular weight on the increase in surface pressure as contrasted with the equal effect of the freons on the decrease in heat transfer with injection. The gases air and argon (mol. wt. 28.9 and 40.0, respectively) show an equivalent effect on the increase in surface pressure, whereas each gas had a distinct effect on the reduction in heat transfer. The inference is that the momentum thickness of the boundary layer for both air and argon injection has the same effective distribution along the body.

Concluding Remarks

Agreement between theory and experiment was good for the stagnation point heat transfer with helium, air, and argon injection. The three freon gases showed an equal effect on the reduction in heat transfer at the stagnation point; whereas theory showed a small molecular weight effect.

The prediction of the heat-transfer distribution was good over the whole cone for argon injection. Predictions of heat transfer on the forebody with and without helium injection were fairly good, and predictions on the afterbody were 40% high with helium injection and about 25% high without injection. The lack of agreement with helium injection reflects the disparity with no injection.

An inviscid surface pressure prediction, which had been coupled to a nonsimilar boundary-layer theory, was generally in good agreement with the measured surface pressure over the whole blunt cone model for helium and argon injection and for no injection.

References

[1] Lewis, C. H., Adams, J. C., and Gilley, G. E., "Effects of Mass Transfer and Chemical Non-equilibrium on Slender Blunted Cone Pressure and Heat Transfer Distribution at $M_\infty = 13.2$," AEDC TR-68-214, Nov. 1968, ARO Inc.

[2] Yoshikawa, K. K., "Linearized Theory of Stagnation Point Heat and Mass Transfer at Hypersonic Speeds," TN D-5246, 1969, NASA.

Influence of Gravity on the Performance of a Conical Vortex Separator

K. R. Burton*
Convair Division of General Dynamics, San Diego, Calif.

Introduction

Vortex separators are widely used for the separation of the phases of a two-phase fluid and consist essentially of a conical channel containing the swirling mixture. The heavy particles are thrown to the wall, where a boundary layer forms in the film of heavy fluid. Due to the potential motion of the bulk of the fluid, a pressure field develops which induces a secondary flow in the boundary layer. It is this phenomenon that causes the flow of heavy fluid toward the small open end of the cone and is responsible for the effectiveness of the vortex separator. A gravity force, depending upon its direction, can either increase or reduce the swirl-induced flow.

Lawler and Ostrach[1] discussed the effect of gravity on vortex separators and defined a Froude number for qualitative analysis of the relative strength of the gravitational and inertial forces. Their analytical results were obtained by considering the body force to act on the heavy fluid, both within and outside the boundary layer. Combining the pressure gradient and body force terms allowed use of Taylor's original solution[2] for boundary-layer motion in a swirling conical flow.

This note differs from Ref. 1 in that the effect of gravity is neglected in the thin region of heavy fluid outside the boundary layer. Such an assumption allows explicit prediction of the effect of a body force on the boundary-layer flow, and results in definition of the limiting condition for use of a vortex separator in an adverse gravity field.

Taylor's Swirl Problem

An incompressible fluid enters a conical tube tangentially at the large end. The conical chamber, whose apex angle is 2α, is so designed that the axial component of velocity is small compared to the swirl component. Except for a thin layer along the wall, the velocity is given by Ω/r, where r is the distance from the axis and Ω is the circulation.

The equations of motion with the usual boundary-layer approximations are listed below, in spherical coordinates, with the origin at the apex of the cone:

$$u\frac{\partial u}{\partial R} + \frac{v}{R}\frac{\partial u}{\partial \theta} - \frac{w^2}{R} = -\frac{1}{\rho}\frac{\partial p}{\partial R} + \frac{\nu}{R^2}\frac{\partial^2 u}{\partial \theta^2} \qquad (1)$$

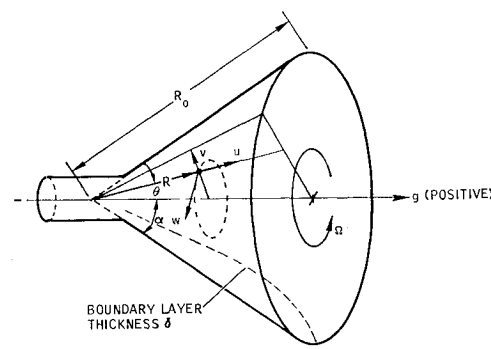

Fig. 1 Coordinate system.

Received August 11, 1969; revision received January 21, 1970. This work was performed under Contract NAS 1-8494, NASA Langley Research Center. The author wishes to acknowledge the helpful suggestions contributed by E. A. Evans.

* Senior Thermodynamics Engineer.

$$0 = (1/\rho R)\,\partial p/\partial\theta \tag{2}$$

$$u\,\partial w/\partial R + (v/R)\,\partial w/\partial\theta + wu/R = (\nu/R^2)\,\partial^2 w/\partial\theta^2 \tag{3}$$

The continuity equation is

$$\partial u/\partial R + 2u/R + (1/R)\,\partial v/\partial\theta = 0 \tag{4}$$

where R is the radial distance from the apex of the cone, θ is the angle a radius vector makes with the axis, u is the radial velocity, v is the component of velocity perpendicular to R, p is the pressure, ρ is the density, and ν is the kinematic viscosity ($\nu = \mu/\rho$). The coordinate system is shown in Fig. 1.

Outside the boundary layer $w = \Omega/R \sin\theta$ and the pressure is given by

$$p/\rho = -\tfrac{1}{2}\,\Omega^2/R^2 \sin^2\theta + \text{const} \tag{5}$$

Inclusion of Gravity Force

We depart from Taylor's equations by including an axial body force which is positive in the direction from the apex to the large end of the cone. The component of this force normal to the wall is neglected and only the fluid in the boundary layer is considered to be influenced by the body force. Such an assumption is appropriate for a vortex separator where the boundary layer consists of fluid with a density greater than the fluid in the core, and very little of the heavy fluid in the separator is found outside the boundary layer. Equation (1) then becomes

$$u\frac{\partial u}{\partial R} + \frac{v}{R}\frac{\partial u}{\partial\theta} - \frac{w^2}{R} = -\frac{1}{\rho}\frac{\partial p}{\partial R} + \frac{\nu}{R^2}\frac{\partial^2 u}{\partial\theta^2} + g\cos\alpha \tag{6}$$

Equations (2–4) are unchanged.

Equations (3) and (6) are integrated over the boundary-layer thickness, from $\theta = \alpha$ to $\theta = \alpha - \delta/R$. By substituting the same velocity distribution expressions as Ref. 2, where $\eta = R(\alpha - \theta)/\delta$, and δ is the boundary-layer thickness, we obtain

$$\frac{\delta^2}{R^2}\left[\left(R\frac{dE^2}{dR} + \frac{RE^2}{2\delta^2}\frac{d\delta^2}{dR} - E^2\right)\int_0^1 f^2 d\eta + K - \int_0^1 \phi^2 d\eta\right] = -E\,\frac{\nu\sin\alpha}{\Omega}\left(\frac{df}{d\eta}\right)_{\eta=0} \tag{7}$$

$$\frac{1}{2}\frac{\delta^2}{R^2}\left(R\frac{dE^2}{dR} + \frac{RE^2}{\delta^2}\frac{d\delta^2}{dR}\right)\left(-\int_0^1 f d\eta + \int_0^1 f\phi d\eta\right) = -E\,\frac{\nu\sin\alpha}{\Omega}\left(\frac{d\phi}{d\eta}\right)_{\eta=0} \tag{8}$$

The nondimensional parameter K is a result of the introduction of the gravity force term and is defined as

$$K \equiv 1 - (gR^3 \sin^2\alpha\cos\alpha)/\Omega^2$$

If the inlet velocity is defined as $W_0 = \Omega/R_0 \sin\alpha$, then the parameter K can be written

$$K = 1 - (\cos\alpha/F)(R/R_0)^3$$

where F, a Froude number, is defined as

$$F \equiv W_0^2/R_0\,g$$

To nondimensionalize Eqs. (7) and (8), introduce

$$\left.\begin{aligned} R_1 &= R/R_0 \\ \delta_1 &= (\delta/R_0)\,(\Omega/\nu\sin\alpha)^{1/2} \end{aligned}\right\} \tag{9}$$

We then arrive at two nonlinear ordinary differential equations with dependent variables E^2 and $E\delta_1^2$ and independent variable R_1

$$dE^2/dR_1 = -[98(1 - GR_1^3)/R_1] + 2E^2/R_1 - 330\,E^2R_1/E\delta_1^2 \tag{10}$$

$$\frac{d}{dR_1}(E\delta_1^2) = \frac{49(1 - GR_1^3)E\delta_1^2}{E^2R_1} - \frac{E\delta_1^2}{R_1} + 285R_1 \tag{11}$$

These differ from Taylor's equations in the term containing G. The factor G is a nondimensional relationship between the swirling inertial force and gravity force and is defined as

$$G \equiv 2.14\cos\alpha/F$$

When $G = 0$ we have Taylor's original pair of equations.

Numerical Analysis and Results

Equations (10) and (11) have been integrated numerically starting at $R_1 = 1 - \Delta$ with the approximate values;

$$E^2 = 19.1\Delta\,(1 - G)$$

$$E\delta_1^2 = -80\Delta$$

A plot of δ_1 vs R_1 for selected G values is given in Fig. 2. The curve for $G = 0$ is in agreement with Ref. 2.

To determine the boundary-layer mass flow rate, we integrate the u-velocity over the boundary-layer thickness:

$$m = 2\pi\rho R^2 \sin\alpha \int_{\theta=\alpha}^{\theta=\alpha-\delta/R} u\,d\theta$$

Using the relationships $d\theta = -(\delta/R)d\eta$,

$$\int_0^1 f(\eta)d\eta = \frac{1}{12}$$

and Eq. (9), we have

$$m = -(\pi/6)\rho R_0 E\delta_1\,(\Omega\nu\sin\alpha)^{1/2}$$

A nondimensional flow rate is defined as

$$M = m[-(\pi/6)\rho R_0]^{-1}(\Omega\nu\sin\alpha)^{-1/2} = E\delta_1$$

Values of $E\delta_1$ as a function of R_1 from the solution of Eqs. (10) and (11) are plotted in Fig. 3.

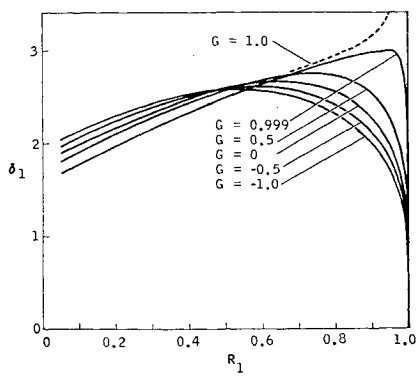

Fig. 2 Effects of gravity parameter G on boundary-layer thickness.

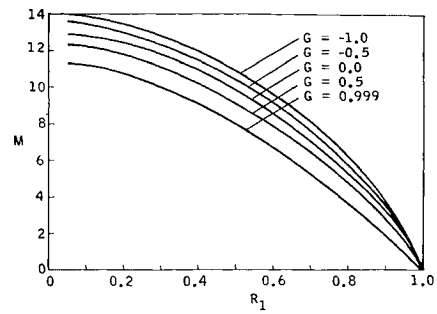

Fig. 3 Effects of gravity parameter G on mass flow rate.

In a favorable gravity field, the heavy fluid can be delivered to the conical tube by gravity from an attached cylinder in which the separation process is concentrated. Under adverse gravity conditions, however, the separation process alone must be relied upon for supply of heavy fluid to the cone. The numerical results show that for values of G greater than 1.0, the boundary-layer flow reverses near the base of the cone, and the heavy fluid cannot be transported by this mechanism toward the apex. Thus, $G = 1.0$ is the limiting condition for operation of a vortex separator in an adverse axial gravity field.

It should be noted that values of G must be determined by using the appropriate value for Ω in the heavy fluid. This can be done by equating shear stress at the interface as in Ref. 1, or by equating pressures and assuming slip at the surface of the heavy fluid.

References

[1] Lawler, M. T. and Ostrach, S., "A Study of Cyclonic Two-Fluid Separation," AFOSR 65-1523, June 1965, Fluid, Thermal and Aerospace Sciences, Engineering Division, Case Institute of Technology, Cleveland, Ohio.

[2] Taylor, G. I., "The Boundary Layer in the Converging Nozzle of a Swirl Atomizer," *Quarterly Journal of Mechanics and Applied Mathematics*, Vol. 3, Pt. 2, June 1950, pp. 129–139.

Covariance Propagation Via Its Eigenvalues and Eigenvectors

G. J. Bierman*
Litton Systems Inc., Woodland Hills, Calif.

Introduction

In many applications of linear filter theory to navigation analysis, it is important to propagate and update the covariance in an accurate fashion. The square root formulations presented in Refs. 1 and 2 were designed to improve accuracy and maintain non-negativity of the covariance during a Kalman update. One must, however, compute a square root covariance at each update; since the covariance itself is propagated in the interim. A notable exception to this occurs when there is no dynamic noise, i.e., Q of Eq. (1) is zero. In this case, the square root may be propagated by means of the transition matrix.[1]

If during the covariance propagation, the accumulated errors (because of the roundoff and/or the propagation algorithm) cause it to lose its semidefinite character, then the square root updating process may fail. Dyer and McReynolds,[4] introduce orthogonal transformations to circumvent the difficulty (of propagating the covariance) when dynamic noise is present. Their analysis was based upon sequential techniques; but, if the dynamics of the problem are time varying, it may be difficult to apply their results.

Andrews[3] presents an algorithm for continuous propagation of a triangular square root by means of differential equations. The differential equations[3] (5) appears difficult to propagate because of the matrix inversion required at each integration step. Further, his proposed update does not preserve the triangular nature of the square root, so that it is necessary to reinitialize the triangular square root after each update.

Received September 18, 1969; revision received February 10, 1970.

* Engineering Specialist, Systems Analysis Department, Guidance and Control Systems Division.

In this Note, we present a method of propagating the covariance by means of differential equations for its time varying eigenvalues and eigenvectors.† Because the eigenvalues are propagation variables, one can arrange the propagation algorithm so that one is assured that the covariance will not lose its positive semidefinite character. In addition, at an update time, one can apply the square root updating procedures suggested in Refs. 2 and 3, since square roots are expressed quite simply in terms of the eigenvector matrix $\mathbf{X}$ and the eigenvalue matrix Λ; i.e., if $C = \mathbf{X}\Lambda\mathbf{X}'$, $\Lambda = \text{Diag}(\lambda_1, \ldots, \lambda_n)$, then $\mathbf{X}\Lambda^{1/2}Y$ is a square root of C where $\Lambda^{1/2} = \text{Diag}(\lambda_1^{1/2}, \ldots, \lambda_n^{1/2})$ and Y is any unitary matrix, because $C = C^{1/2}(C^{1/2})'$. It is hoped that the time history of the eigenvalues and principal axes will give further insight into the dynamics of the linear analysis.

Derivation of the Differential Equations Governing the Eigenvectors and Eigenvalues of the Covariance

The covariance matrix we are concerned with can be defined as the solution to

$$\dot{C} = AC + (AC)' + Q, \quad C(O) = C_0 \tag{1}$$

A is an $n \times n$ time varying matrix; C_0 and Q are symmetric $n \times n$ matrices; $(\dot{})$ represents time derivative; and the $(')$ denotes matrix transpose. The time argument is omitted for ease of notation.

As pointed out in Bellantoni and Dodge,[2] one may represent C by

$$C = \mathbf{X}\Lambda\mathbf{X}', \quad \mathbf{X} = (\mathbf{X}_1, \ldots, \mathbf{X}_n) \tag{2}$$

where Λ is a diagonal matrix whose elements are the eigenvalues of C, and the columns of $\mathbf{X}$ are the orthonormal eigenvectors corresponding to these eigenvalues. From its definition we have

$$\mathbf{X}\mathbf{X}' = E - \text{identity} \tag{3}$$

and consequently,

$$\dot{\mathbf{X}}\mathbf{X}' + \mathbf{X}\dot{\mathbf{X}}' = 0 \tag{4}$$

Therefore,

$$\dot{\mathbf{X}} = \mathbf{X}\Gamma, \quad \Gamma = -\dot{\mathbf{X}}'\mathbf{X} \tag{5}$$

Equation (5) reflects the fact that the columns of $\dot{\mathbf{X}}$ are linear combinations of the basis unit vectors $\mathbf{X}_1, \ldots, \mathbf{X}_n$. Further, applying Eqs. (3) and (4) to Eq. (5) results in

$$\Gamma = -(\mathbf{X}\Gamma)'\mathbf{X} = -\Gamma' \tag{6}$$

i.e., Γ is skew-symmetric.

Let us now exploit the relationship involving $\mathbf{X}$, Λ, and C, Eq. (2). Consider the following self-explanatory equations:

$$\begin{aligned} \Lambda &= \mathbf{X}'C\mathbf{X} \\ \dot{\Lambda} &= \dot{\mathbf{X}}'C\mathbf{X} + \mathbf{X}'\dot{C}\mathbf{X} + \mathbf{X}'C\dot{\mathbf{X}} \\ \dot{\Lambda} &= \Gamma'\mathbf{X}'C\mathbf{X} + \mathbf{X}'\dot{C}\mathbf{X} + \mathbf{X}'C\mathbf{X}\Gamma \\ \dot{\Lambda} &= -\Gamma\Lambda + \mathbf{X}'\dot{C}\mathbf{X} + \Lambda\Gamma \end{aligned} \tag{7}$$

Because of Eq. (6), the diagonal elements of Γ are zero, so that the diagonal terms of Eq. (7) are

$$\dot{\lambda}_i = \mathbf{X}'_i\dot{C}\mathbf{X}_i, \; i = 1, \ldots, n \tag{8}$$

These are the required differential equations for eigenvalue propagation.

In the previous paragraph, the diagonal elements of Eq. (7) were equated and this led to the differential equations for the eigenvalues, Eq. (8). Equating the off-diagonal elements will result in the evaluation of the Γ_{ij} which define the differ-

† The derivation is patterned after that given by Kalaba et al. in Ref. 5.